Development of an anti-aging formulation based in nanotechnology capable of balancing the cutaneous microbiome

Alexandra Lan[1], Wenjia Yu[1], Jie Kong[1], Chenxi Bao[1], Qingyang Meng[1], Li Chen[1], Zhenxiang Lin[1], Siqueira, Raquel A. G. B.[2]; Britto, Nicoly T. R.[2]; Santos, Yasmin R.[2], Sposaro, Fabiana R.[2]; Pequeno, Ana Luiza V.[3]; Leite-Silva, Vânia R.[2,4], Bagatin, Edileia[3], Andreo-Filho, Newton [2], **Lopes, Patricia S.[2*]**

[1]Shanghai Pechoin Daily Chemical Corporation, Shanghai 200060, China;

[2]Departamento de Ciências Farmacêuticas, Instituto de Ciências Ambientais, Químicas e Farmacêuticas, Universidade Federal de São Paulo, UNIFESP - Diadema, Brazil;

[3]Departamento de Dermatologia, Escola Paulista de Medicina, Universidade Federal de São Paulo, UNIFESP – São Paulo, Brazil;

[4]Therapeutics Research Centre, The University of Queensland Diamantina Institute, Translational Research Institute, Brisbane, Queensland 4102, Australia.

*Patricia S. Lopes, Rua São Nicolau 210 – CEP 09913030 – Diadema, São Paulo, Brazil, 55 11 995272057, patricia.lopes@unifesp.br

Abstract

Human skin hosts a diverse microbiota that influences body homeostasis and protection, as imbalances can lead to skin diseases and aging. A new cosmetic formulation enriched with a postbiotic lipid nanocarrier (NLCp) to prevent skin aging by rebalancing the skin microbiota. NLCp (4% w/w) was prepared by microemulsification followed by phase inversion, added to a semi-solid formulation assessed over 90 days for rheological behavior,

pH, and particle size distribution (PSD). A 3D skin model was used to assess safety and efficacy *in vitro*. An *in vivo* study with 40 participants (aged 25-35 and 35-45 years) compared the formulation (DF) to a control (CF). Hydration, oiliness, transepidermal water loss, pH, microbiome metagenomics, and clinical evaluations were analyzed from 0 to 120 days. NLCp had a mean size of 200 nm and a span of 1.58. PSD and pH were stable over 60 days. Rheological behavior was pseudoplastic, suitable for topical use. *In vitro* results showed that DF did not induce IL-6, IL-8, or TNF-α, and increased aquaporin-3 (101.4%), involucrin (56%), filaggrin (93%), SIRT-1 (165.5%), FoxO3 (40.3%), collagen synthesis (89.9%), and antioxidant effects (92.9%). *In vivo* tests showed significant hydration increases at 60 and 90 days with DF, corroborant *in vitro* results. Clinical evaluation reported improvements in facial brightness, skin uniformity, and blemish lightening. DF enhanced hydration, barrier integrity, antioxidant effects, and collagen synthesis, effectively delaying signs of aging. Additionally, it improved the appearance of wrinkles, controlled the presence of *Corynebacterium* species, and balanced *Cutibacterium acnes*, promoting overall skin health.

Keywords: Nanotechnology; Microbiome balance; Innovation; Antiaging; Skin Microbiota

1. INTRODUCTION

Skin aging results from the combination of intrinsic and extrinsic factors and is influenced by the dysbiosis of the skin microbiome. The microbiome includes the interaction between the human genome and microorganisms, particularly bacteria, as well as viruses and fungi. There is a mutualistic relationship where the host provides nutrients, and microorganisms offer protection against pathogens [1]. Bacteria, despite comprising only 0.1% of the microbiota, are the most relevant [2]. Metagenomic sequencing studies of 16S ribosomal RNA have identified the skin microbiome's bacteria, classified into four phyla: Actinobacteria, Firmicutes, Bacteroidetes, and Proteobacteria, which are also found in the gastrointestinal tract in different proportions.

Disturbance in the balance between the host and the microbiome, known as dysbiosis, reduces bacterial diversity and is a focus for new therapeutics [3,4,5]. Preventing skin aging involves controlling intrinsic factors related to cellular senescence and extrinsic factors, particularly photoprotection and hydration [6]. Recent studies highlight the role of topical postbiotics in daily skincare and treating various dermatoses by promoting a positive bacterial balance in the skin microbiota [7].

In this context, the aim of this work was to develop an innovative cosmetic product containing prebiotics and a nanostructured postbiotics able to restore the balance of the microbiome reducing the aged facial skin signals.

2. MATERIALS AND METHODS

2.1 Development of lipid nanoparticles

Nanostructured Lipid Carrier (NLC) were prepared using an exclusive low energy microemulsification method. The formulation consisted of a lipid phase, an ethoxylated fatty alcohol surfactant, a co-surfactant and a hydrophilic dispersion polymer. The development of the nanoparticles began with selecting the best co-surfactant and dispersion polymer, followed by the incorporation of postbiotics (long, medium and short-chain fatty acids). The particle size distribution was determined using static light scattering (laser diffraction) for 90-day stability period at different temperatures: 8º, room temperature (R.T) and 40º C.

2.2 Control and Developed Formulation Preparation

A cosmetic emulsion base with 6% w/w of free space was used to prepare the Control Formulation (CF) and the Developed Formulation (DF). In the CF, the free space of the cosmetic emulsion base was completed with water under stirring at 80 rpm in a pilot reactor (RORENOX, SA, Brazil), at 23ºC. The DF was prepared in same pilot reactor and conditions, where 4% w/w of NLC and dispersion of 0.5% w/w of *alpha-glucan oligosaccharide (and) Polymnia sonchifolia*

root juice (and) Maltodextrin (and) Lactobacillus, shortly APML, in 1.5% w/w of water was separately incorporated into the cosmetic emulsion base.

2.2.1 Stability assays

The result formulations were submitted to different storage conditions (8°C, room temperature [R.T.], and 40°C) for 90 days. Particle Size Distribution (PSD), pH, and viscosity curves (0.1 – 50 s^{-1}) were analyzed at 7, 15, 30, 60, and 90 days. In the CILAS 1190 Particle Analyzer, based on the SLS principle. The Lorenz-Mie theory was applied as the measurement principle, and readings were taken in triplicate [8]. Samples were dispersed in water (10%) and analyzed in a digital pHmeter (HANNA 21) in triplicate [9]. In the Modular Compact Rheometer MCR 92 (Anton Paar), a 25 mm plate-plate geometry was used to evaluate the viscosity curve of the samples. Ascending curves were generated as a function of shear rate (0.01 – 50 s^{-1}), with measurements taken every 3 seconds and a 1.0 mm gap at 25°C [10].

2.3 Efficacy and Safety in 3D equivalent skin models

For *in vitro* safety and efficacy evaluation, the formulations were tested using 3D equivalent skin models and cytotoxicity parameters (vital dye incorporation or RNA assessment). In the three-dimensional cell culture, fibroblasts were embedded in a protein matrix and on the surface of this matrix, keratinocytes were added to form the dermis and epidermis for the equivalent skin model. Briefly, the solutions containing the control (CF) and sample groups (DF) were applied to the surface of the skin model equivalently every two days for seven days. Messenger RNA was extracted with Trizol, evaluating its quantity and purity for each group. From the extraction of messenger RNA, the reverse transcriptase reaction was performed to obtain the complementary DNA strand. Next, analysis of the expression of aquaporin-3, involucrin, filaggrin, interleukin-6, interleukin-8, TNF-α, FoxO3, SIRT-1, collagen and NRF2 was performed. The GAPDH marker was used as an endogenous control. The results were evaluated using Microsoft Excel and Graphpad Prism software. For the analysis of data obtained by RTq-PCR, analysis based on 2^-ΔΔCt was used to graphically represent the relative expression by fold-change and statistical

analysis based on ΔCt data. The positive control to aquaporin-3, filaggrin and involucrin was D-pantenol, for the Interleukins was SDS and for FoxO3, Sirt-1, collagen and NRF-2 was Resveratrol. Statistical analysis for comparison between groups was performed using the One-way Anova test and a level of statistical significance considered lower than 0.05.

2.4. In vivo Cutaneous Biometrology and Clinical evaluation

A pilot, proof-of-concept, therapeutic intervention, prospective, randomized, placebo-controlled, parallel-group clinical study was conducted to evaluate the efficacy and safety of an innovative nanostructured topical formulation containing prebiotics and postbiotics for aging facial skin. The research project was approved by the Research Ethics Committee at UNIFESP (CAAE: 74030523.0.0000.5505), and included 40 women, aged 25 to 45, with mild to moderate facial aging (GLOGAU grades II and III) [11]. Participants were recruited through the intranet/UNIFESP, the Dermatology Outpatient Clinic of EPM/UNIFESP, the University Hospital 2 (HU2), the NASF (Employee Health Assistance Center), or through spontaneous inquiry at HU2. Twenty participants were between 25 and 35 years old, and the other 20 were between 36 and 45 years old.

Participants were randomized into two groups, receiving either the Control Formulation (CF) or the Developed Formulation (DF), applied twice daily for three months. They maintained their usual skincare routine, adding only CF or DF.

Clinical parameters included changes in the skin microbiome, evaluated via forehead swabs taken at the same location, marked, and photographed during all five scheduled visits. Participant feedback and evaluations by the researcher and two independent dermatologists were conducted using photographs captured by VISIA™ (Canfield, USA). Observations were rated on a 5-point Likert scale: 1 (much worse) to 5 (much better).

Additional assessments included the SCINEXA classification score and measurements of skin hydration using corneometry (Corneometer™), transepidermal water loss (TEWLmeter™), pH (pHmeter™), Sebumeter™ and profilometry using Visioscan™ (all from Courage&Khazaka-

Germany). High-frequency ultrasound (DermaScan™), from Cortex Technology, Denmark, was used to assess the subepidermal low-echogenic band (SLEB) and dermal echogenicity. These parameters were evaluated twice: before and after the treatment.

2.5 Metagenomic Analysis of Skin Microbiome Samples

Briefly the method followed [12] where the bacterial composition analysis was performed with the Illumina® Nextseq™. DNA was isolated from swabs using a ZymoBIOMICS® DNA Miniprep Kit (Zymo Research, Irvine, CA) due to the low biomass, resulting in more concentrated DNA. Bacterial 16S ribosomal RNA gene targeted sequencing was performed using the Quick-16S™ NGS Library Prep Kit (Zymo Research, Irvine, CA). The bacterial 16S primers amplified the V3-V4 region of the 16S rRNA gene. The final pooled library was cleaned with the Select-a-Size DNA Clean & Concentrator™ (Zymo Research, Irvine, CA), then quantified with TapeStation®(Agilent Technologies, Santa Clara, CA) and Qubit® (Thermo Fisher Scientific, Waltham, WA). The final library was sequenced on Illumina® Nextseq™ with a P1 reagent kit (600 cycles). The sequencing was performed with 30% PhiX spike-in.

2.6 Statistical analysis plan

The results were subjected to statistical analysis using Analysis of Variance to verify the existence of differences between the formulations for a significance level of 0.05 (a = 0.05). Once the existence of differences was verified, the Tukey test was applied to group the formulations to identify the set of strategies that best leads to a desired response factor.

3. RESULTS AND DISCUSSION

Formulation Development

The analysis of nanoparticle size using laser diffraction provided results for d10, d50, and d90 (representing the diameters at percentage of particles), the percentage of particles with a diameter less than or equal to 500 nm (% p ≤ 500 nm), average diameter, dispersity (SPAM), and uniformity ratio (RU). These values are detailed in Table I. Additionally, Figure 1 shows the

particle size distribution in terms of volume of particles. In summary, the average diameter of the nanoparticles was initially 210 nm with a dispersity (SPAM) of 2.06.

Nanoparticles	**Size values (µm) ± SD**					
Dispersion	**%p≤500 nm**	**d10**	**d50**	**d90**	**dm**	**SPAM**
Passing Volume	94.82 ± 0.06	0.06 ± 0	0.17 ± 0	0.41 ± 0	0.21 ± 0	2.06 ± 0
Passing Number	99.92 ± 0.01	0.03 ± 0	0.05 ± 0.01	0.09 ± 0.01	0.06 ± 0.01	1.19 ± 0.02
Uniformity ratio (RU)	3.33 ± 0.29					

Table I- Size distribution of lipid nanoparticles containing fatty acids as postbiotics.

The stability study showed that the formulation is more stable at a temperature of 8°C, maintaining an average diameter of less than 250 nm.

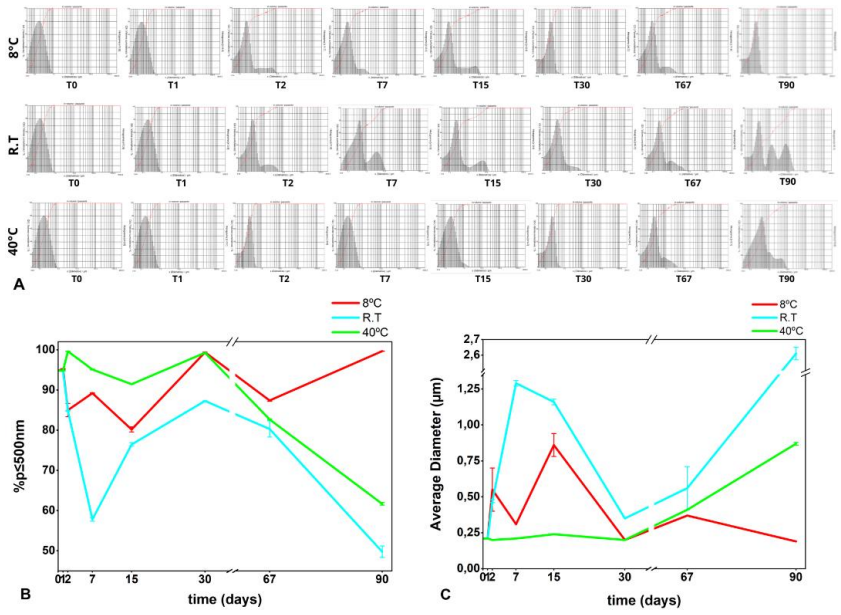

Figure 1. Particle size distribution obtained by laser diffraction technique, expressed in volume of particles and stability at different temperatures for 90 days.

CF and DF remained physicochemical stable throughout all the stability assays and showed non-Newtonian behavior in viscosity curves, considered suitable for cosmetics applications [13] (Fig 2). The incorporation of NLC and *APML* in DF influenced the viscosity, PSD, and pH analyses, showing lower values in comparison of CF.

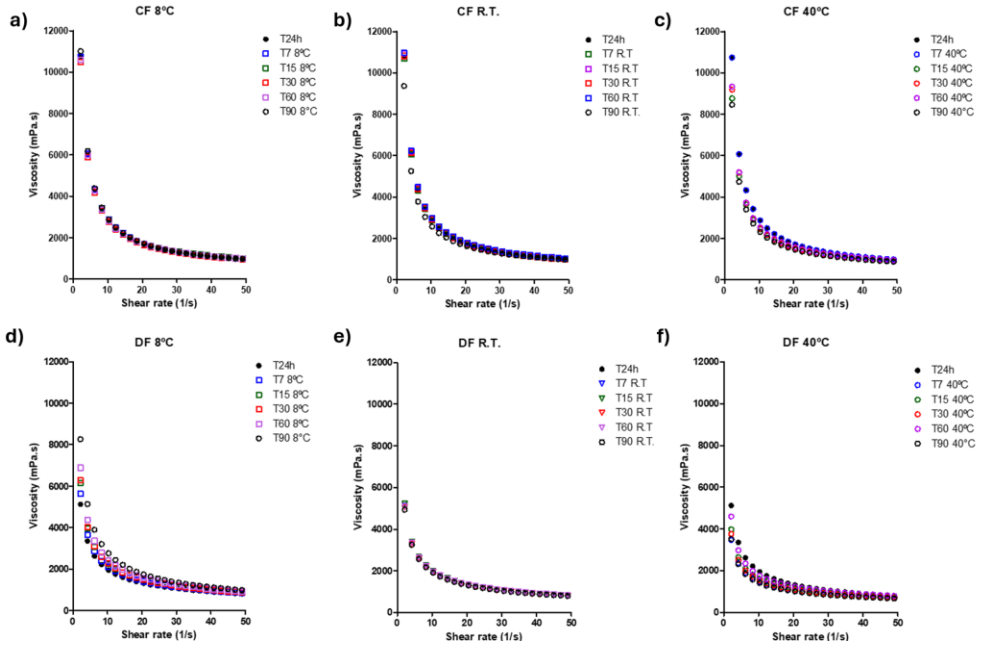

Figure 2 . Viscosity curves of CF and DF at 8°C, R.T, and 40°C during 90 days of stabiliy. Viscosity curves during the stability assay of CF at 8°C (a), R.T. (b), and 40°C (c), and viscosity curves of DF at 8°C (d), R.T. (e), and 40°C (f).

In Figure 3, the PSD of the samples submitted at 8°C and 40 °C showed the most differences for 90 days, while in R.T. the DF did not show a great variation. The pH of CF increased during the stability, and DF remained close to 6.25 and 6.50.

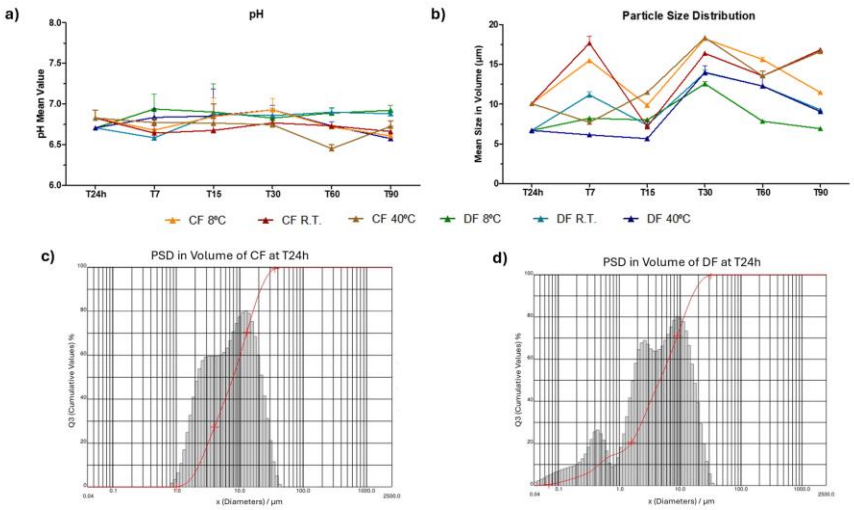

Figure 3. pH and PSD mean values of CF and DF at 8°C, R.T, and 40°C during 90 days of stabiliy. pH (a), PSD values of CF and DF during the stability assay at different storage conditions (b), and histogram of PSD of CF (c) and DF (d) at 24h after development.

3D skin equivalent assays

Exposure of the skin to chemicals, drugs, or cosmetics can result in a wide range of reactions, and this must be assessed before the clinical use of the CF and DF. Therefore, it is crucial to identify chemicals or/and formulations that induce skin irritation and/or sensitization. Also, the *in vitro* tests show the efficacy of the DF. The results of the *in vitro* tests conducted in this research are summarized as follows (Fig. 4).

The relative expression analysis of aquaporin-3 (Fig. 4A) shows a statistically significant increase in the expression of aquaporin-3 in both CF (36.6%) and DF (101.4%). The positive control used in this test was D-Panthenol. It is important to note that the most abundant aquaporin present in the skin, specifically in the plasma membrane of epidermal keratinocytes, is aquaporin-3 (AQP3), which transports both water and glycerol [14].

The results presented in Figure 4B show a statistically significant increase in the expression of Type I Collagen in DF (89.9%) compared to CF (21.5%). Similar behavior was observed with filaggrin (Fig. 4C), where DF showed an 88% increase compared to CF's 5%, and with SIRT-1 (Fig. 4E), where DF presented an increase of 108.6% compared to CF's 11.2%.

In Figure 4D, which relates to involucrin expression, CF and DF did not show a statistically significant difference, although the gene expression levels were different (CF = 4.0%, DF = 40.2%). The results related to FOXO3 (Fig. 4F) also did not show a statistically significant difference, despite the expressive difference in values (CF = 9.5%, DF = 20.9%).Finally, for the antioxidant potential—Nrf-2, DF (84.7%) was statistically different (***p<0.001) compared to the basal control and CF (12.4%), showing an increase in the expression of Nrf-2 and potential antioxidant action.These results indicate that DF presents a better performance than CF.

The interleukin gene expression analysis shows that the DF formulation has a dermo-calming effect compared to the CF. In Fig. 4H, the expression of IL-6 in DF decreased by 65.2% compared to the basal control group and is significantly different from the CF. IL-8 (Fig. 4I) also decreased in DF (74.6%) when compared to the positive control, although this reduction is not statistically significant. Finally, TNF-α (Fig. 4J) follows the same pattern as IL-8, with a 12% reduction in DF compared to the positive control.

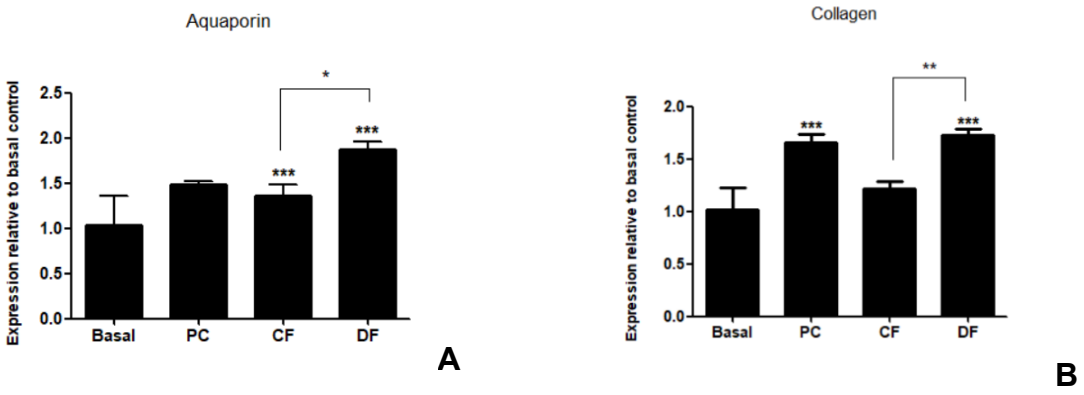

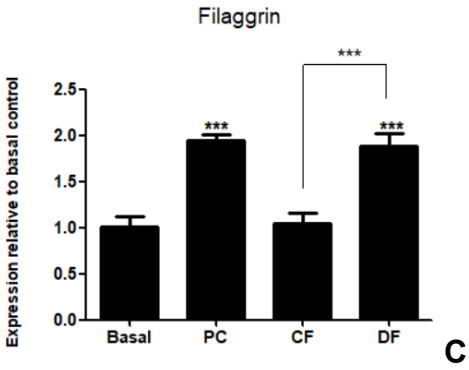
Filaggrin
Expression relative to basal control
2.5
2.0
1.5
1.0
0.5
0.0
***
***
***
Basal
PC
CF
DF

C

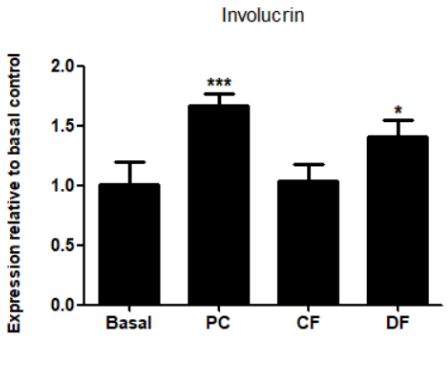
Involucrin
Expression relative to basal control
2.0
1.5
1.0
0.5
0.0
***
*
Basal
PC
CF
DF

D

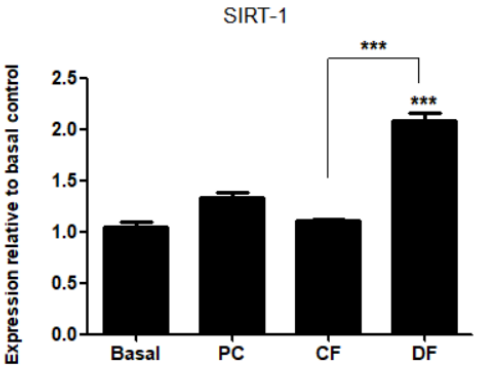
SIRT-1
Expression relative to basal control
2.5
2.0
1.5
1.0
0.5
0.0
***
***
Basal
PC
CF
DF

E

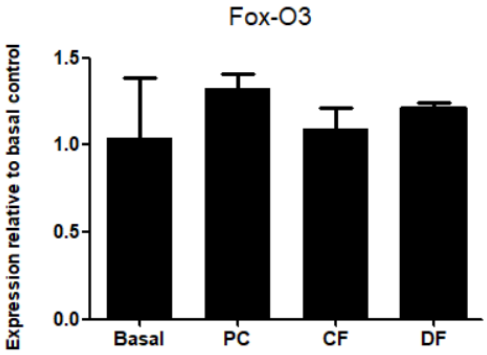
Fox-O3
Expression relative to basal control
1.5
1.0
0.5
0.0
Basal
PC
CF
DF

F

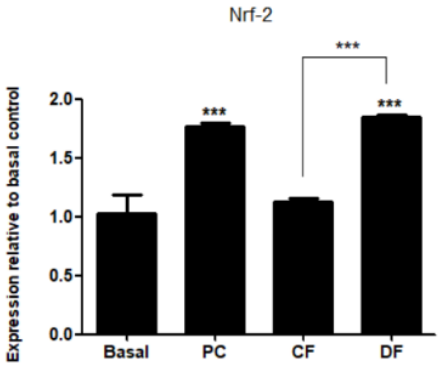
Nrf-2
Expression relative to basal control
2.0
1.5
1.0
0.5
0.0
***
***
***
Basal
PC
CF
DF

G

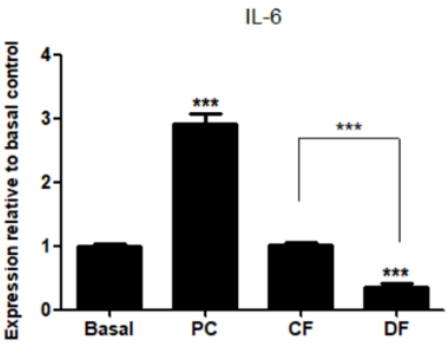
IL-6
Expression relative to basal control
4
3
2
1
0
***
***
***
Basal
PC
CF
DF

H

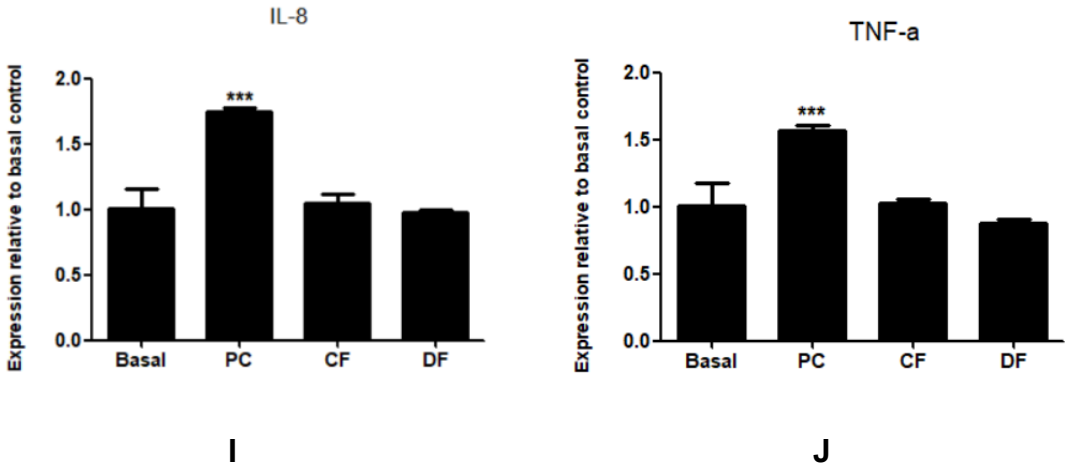

Figure 4. Results of the in vitro tests conducted to assess the efficacy and safety of CF and DF, using skin equivalent 3D models and RTq-PCR analysis. (A) Aquaporin; (B) type I collagen; (C) Fillagrin; (D) Involucrin; (E) Sirt -1; (F) FOX O3; (G) Antioxidant Potential. (H) IL-6; (I) IL-8; (J) TNF-α. Statistical significance was represented as *: p <0.05; **: p<0.01; ***: p<0.001

In vivo tests

The *in vivo* skin cutaneous biophysical parameters considered in this study were measurements of skin hydration using corneometry, transepidermal water loss (TEWLmeter™), pH (pHmeter™), and profilometry (Visioscan™), which evaluates the depth of skin lines and grooves. High-frequency ultrasound (DermaScan™) was used to assess the subepidermal low-echogenic band (SLEB) and dermal echogenicity. Figure 5 shows the results obtained for the forehead at all the tested times t0, T30, T60, T90 and after 1 month without the use of the product (T120). The average of the values of the forty selected subjects with the standard deviation was reported.

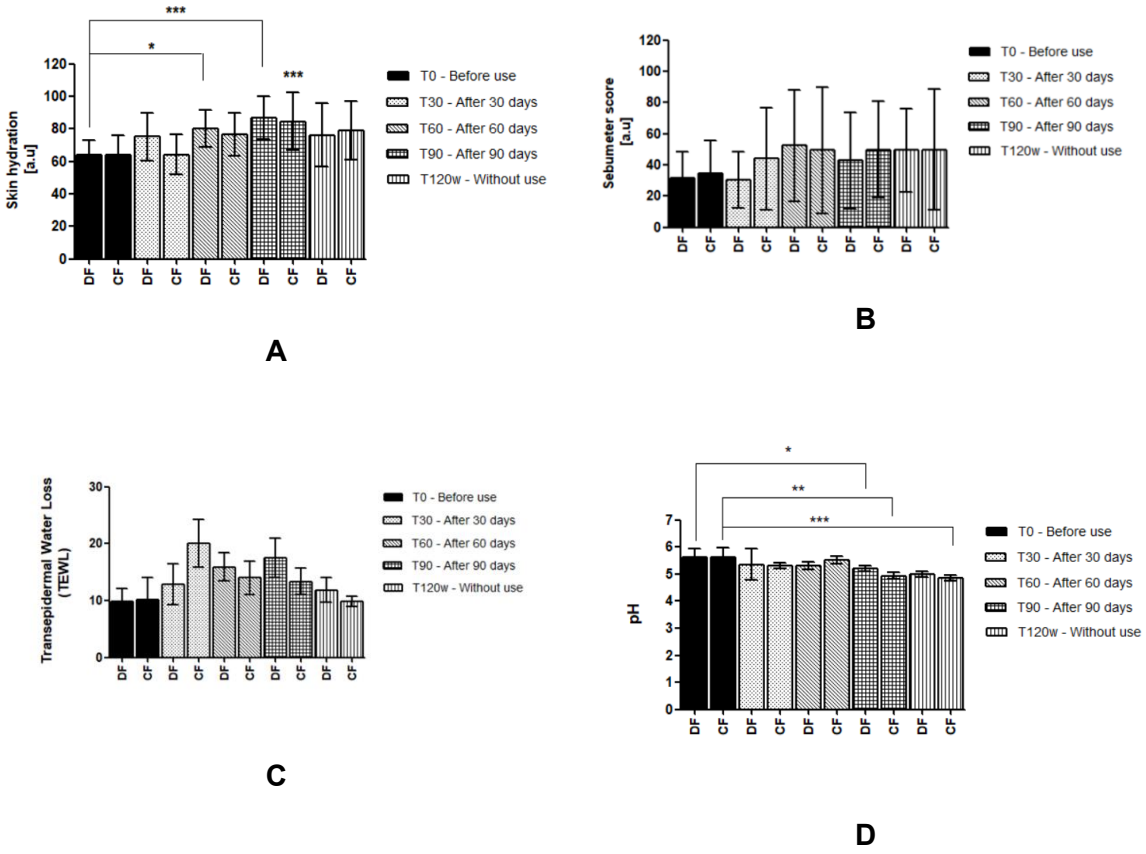

Figure 5. Results concerning instrumental analysis of skin parameters. Samples were taken at time zero (T0) and T30, T60, T90 and T120 days on the forehead area expressed as a mean and standard deviation. Statistical significance at $p < 0.05$ (*), $p < 0.01$ (**), and $p < 0.001$ (***). (A) corneometer; (B) sebumeter; (C) Tewlmeter; (D) pHmeter.

The results shows that skin parameters remain quite constant over time for the panel of volunteers both for CF and DF, specifically for the TEWL values (Fig.5C) showing that DF is not an occlusive formulation nor damage the skin barrier. Sebumeter values (Fig 5B) do not present statistically significant differences.

Moreover, focusing on the Corneometer results (Fig.5A) the results showed that DF is capable to increase hydration after 60 days whereas CF present these same results only at 90 days.

The results regarding the pHmeter values (Fig.5D) showed that DF and CF were able to maintain the skin pH at the normal range during all the tests. The physiological pH of the stratum corneum is usually between 4.1 a 5.8 [15].

Regarding the results obtained with the Visioscan™, Skin smoothness, skin roughness, scaliness and wrinkles were described quantitatively and qualitatively, measured by a special UV-light video and camera (Visioscans VC™, Courage & Khazaka). The images of the skin surface are elaborated by a software so before and after treatment comparisons of the same skin site enable a comparison of trends in skin condition [16]. Figure 6 shows the comparison of these parameters at both age ranges.

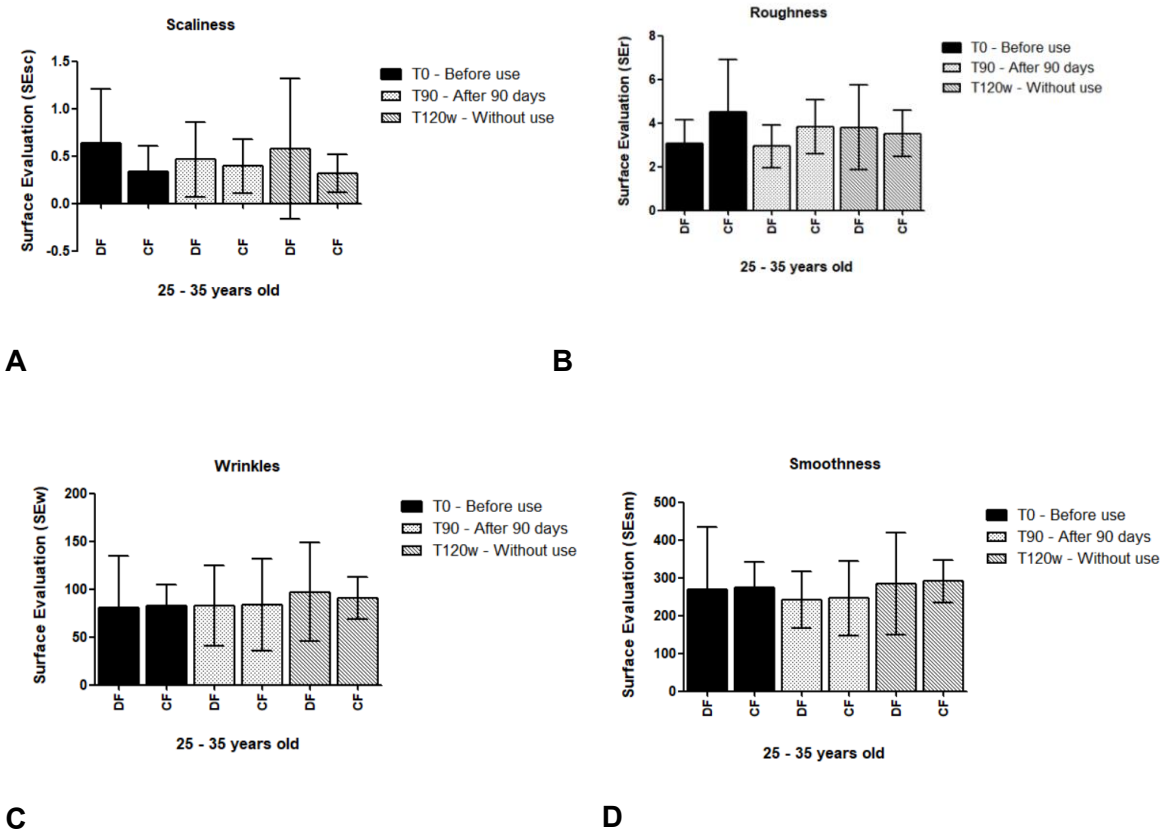

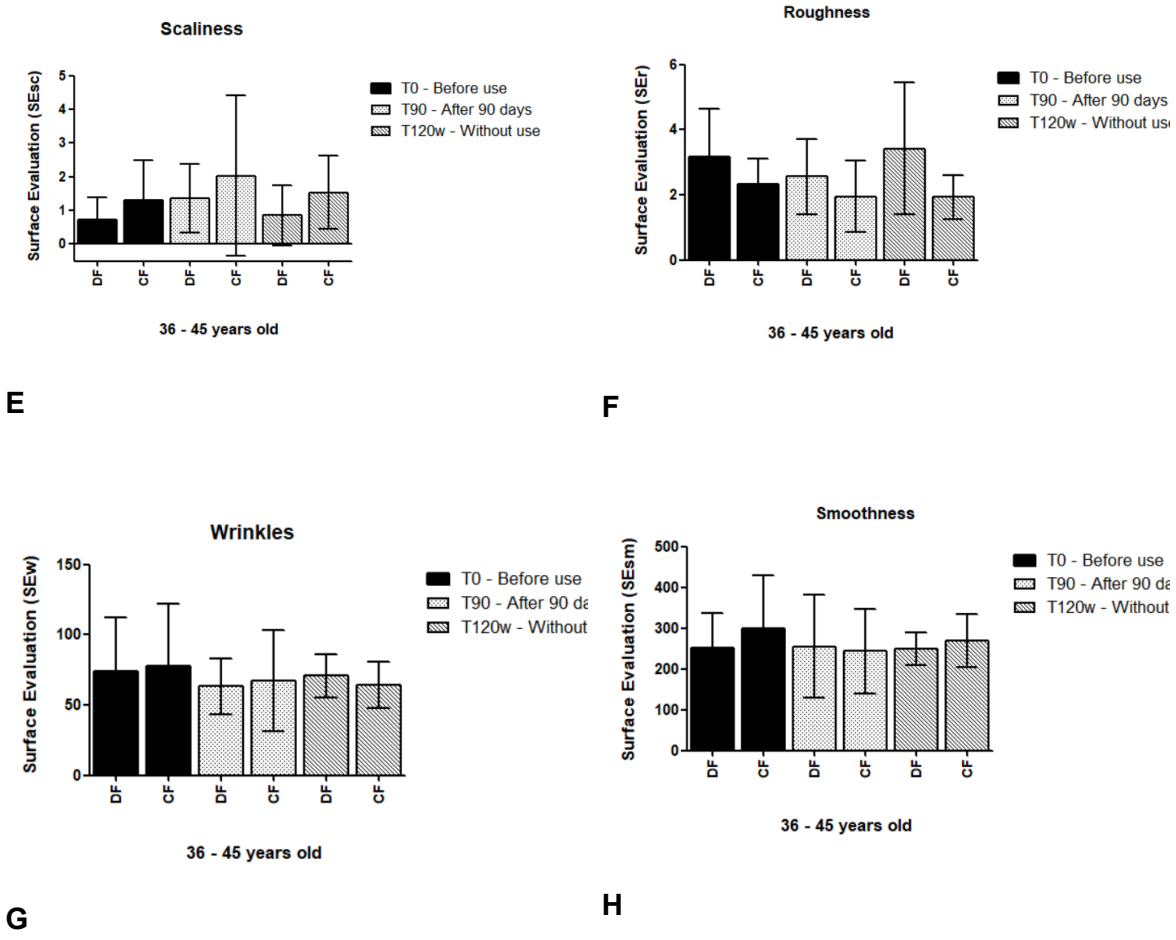

Figure 6. Quantitative results obtained with Visioscan™ at the two different age ranges. (A) scaliness 25-35 years old; (B) roughness 25-35 years old; (C) wrinkles 25-35 years old; (D) smoothness 25-35 years old; (E) scaliness 36-45 years old; (F) roughness 36-45 years old; (G) wrinkles 36-45 years old; (H) smoothness 36-45 years old.

Using a Visioscan VC™, skin can be optically monitored with a method called Surface Evaluation of the LivingSkin (SELS). Skin smoothness (SEsm) is calculated from the average width and depth of wrinkles. Skin roughness (SEr) is the opposite parameter, indicating the skin's texture. Scaliness (SEsc) measures the dryness level of the stratum corneum. Wrinkles (SEw) are assessed based on the proportion of horizontal and vertical wrinkles (Berardesca et al., 2006).

For the 25 to 35 year old group, the results with the formulation (DF) in T90 when compared to T0 were: Scalines is better (reduced); Roughness is equal (same level); Wrinkles got worse (increased slightly) and Smoothness got worse (decreased). For the 36 to 45 year old group, the results with the T90 formulation when compared to T0 were: Scalines worsened (increased); Roughness improved (decreased); Wrinkles improved (decreased) and Smoothness is equal (same level).

It is important to note that the Standart deviation is high, so we do not find any statiscally significant results, but the data leads to conclude that the more mature skin responded more effectively to the formulation developed in most parameters.

One of the modern high-resolution digital camera system is called Visia™ and was used for facial capture and analysis. The Visia™ is a commercialised clinical imaging device that could display eight skin characteristics, as spots on the skin surface that are brown or red marks, wrinkles in the skin such as fine lines or deeper folds, skin texture recorded as raised or depressed surface areas, pores visible as circular openings in the skin, UV spots indicating sun damage due to absorption of UV light by epidermal melanin, brown spots that display any brown mark on the skin either as a natural brown mark or a sun damage, red areas that can display blood vessels and haemoglobin and can be related to a variety of skin conditions and porphyrins, which are the bacterial excretions, found in the pores, and could be related to *Cultibacterium acnes* [17]. The results of this analysis in the subjects are exemplified at Figure 7.


A

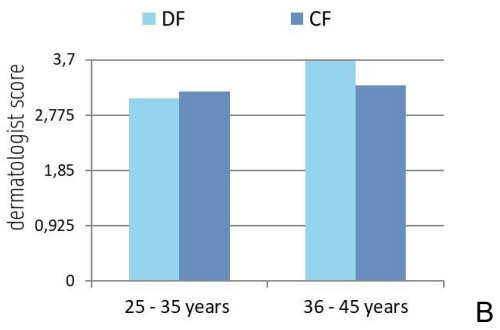

B

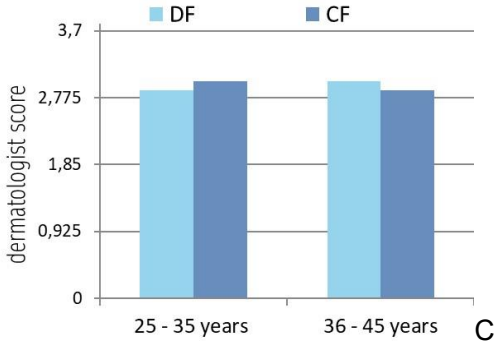

C

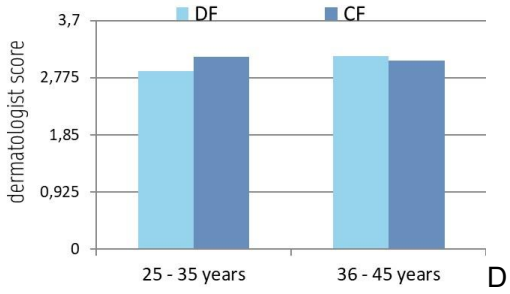

D

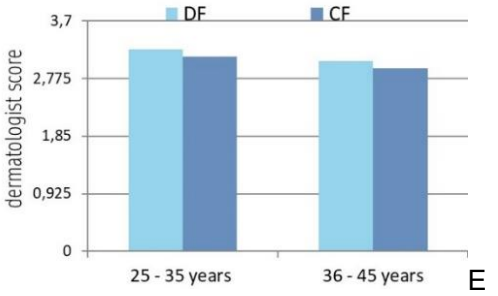

E

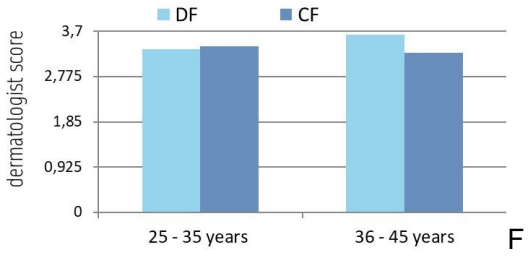

F

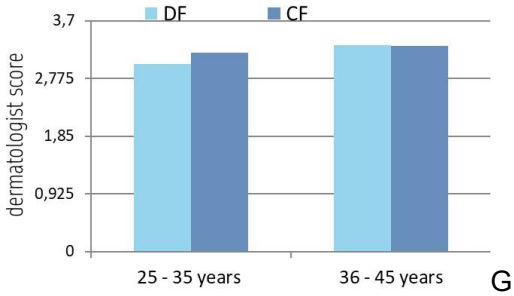

G

Figure 7. Example of the results obtained with Visia™ device showing standart flashlight, UV light and cross polarized flashlight. (A); (B) standard flashlight T90; (C) standard flashlight T120; (D) UV light T90; (E)

UV light T120; (F) cross-polarized flashlight T90; (G) cross-polarized flashlight T120 related to both age range. Scores considered: 1- much worse; 2- worse; 3- equal; 4- better; 5- much better.

A standard flashlight was used to quantitatively analyze the spot, texture, wrinkle, and pore, whereas an UV flashlight was used to analyze the UV spot and porphyrin. Through Canfield's patented RBX™ technique, the brown spot and red area can be observed using a cross-polarized flashlight. When taking the pictures, the camera with a resolution of 15 million pixels can be autofocused [18].

In this context it is possible to infer that DF improves the wrinkles and texture at the age range of 36-45 years old (Fig.7B) for both T90 and T120 days. Finally the DF improved the subsurface red and brown features that enables the visalization of conditions such as rosacea, spider veins, melasma, and acne at the older range both for T90 (Fig.7F) and T120 days (Fig.7G).

The DermaScan™ could identify an important parameter known as the characteristic low echogenic band just beneath the epidermis, known as the "subepidermal low echogenicity band" (SLEB). The aging process involves a decreased amount of water in the dermis due, in part, to the loss of the proteoglycans' hydrophilic properties to retain water. With this alteration, proteoglycans accumulate in the papillary dermis, which reduces echogenicity in that area [19]. SLEB thickness rises linearly with age, serving as a valuable marker of skin ageing. The results obtained with this tecnhique could be found at Figure 8.

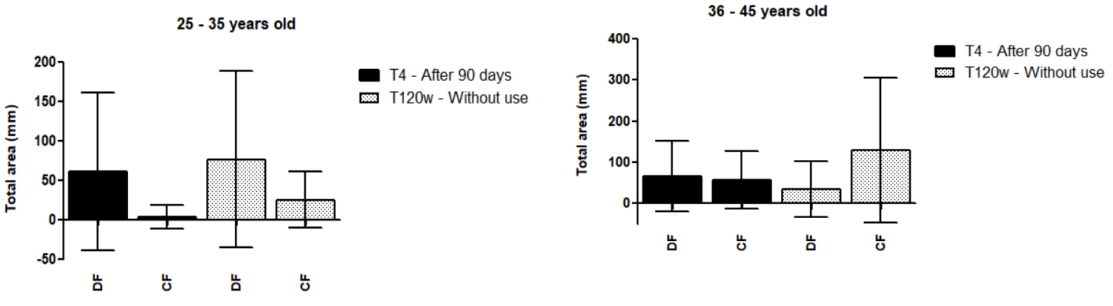

A

B

Figure 8. Results obtained using DermaScan™ both at (A) 25-35 years old range and (B) 36-45 years old range.

It is possible to note an increased at the dermal thickening for the DF at the 25-35 years old range and the increased of dermal echogenicity assessed by high-frequency ultrasound (Figure 8A).

Microbiome analysis

The metagenomics analysys related to the Microbiome is showed at figure 9 and 10.

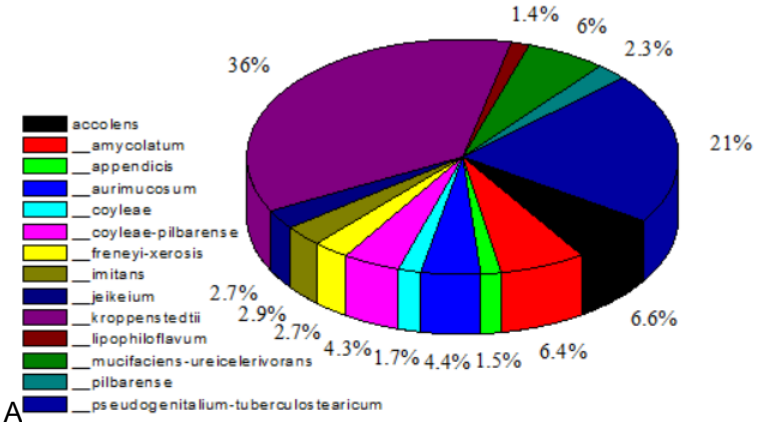

A

B

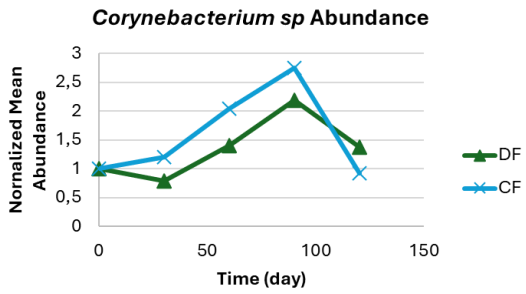

C

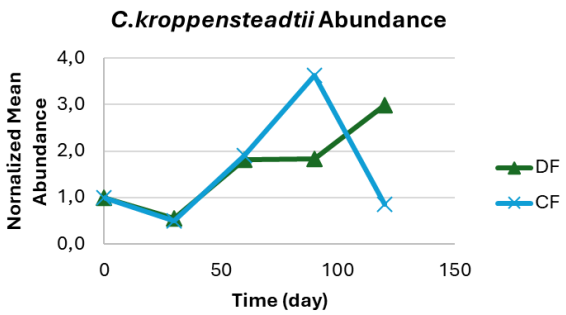

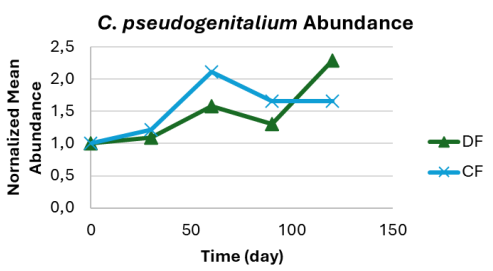

D

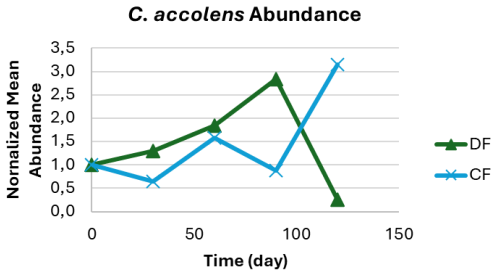

E

Figure 9. Results from metagenomics analysys regarding Corynebacterium sp presence with the most prevalent species. (A). (B) presence of Corynebacterium sp abundance related to DF and CF; (C) presence of Corynebacterium kroppensteadtii abundance related to DF and CF; (D) presence of Corynebacterium pseudogenitalium-tuberculostearicum abundance related to DF and CF; (E) presence of Corynebacterium accolens abundance related to DF and CF.

The composition of skin microbial communities has been extensively shown to depend on the physiology of the skin site, with variations in the relative abundance of bacterial taxa linked to moist, dry, and sebaceous environments. Sebaceous sites are primarily dominated by lipophilic *Cutibacterium* species, whereas bacteria that thrive in humid environments, such as *Staphylococc*us and *Corynebacterium* species, are more abundant in moist areas [20].

It is interesting to note that one of the most prevalent species of *Corynebacterium* sp (figure 9B) is *Corynebacterium kroppenstedtii*, although we found 75 species in all our study (figure 9A). Garlet et al. [20] also found that correlation in their study, and related that this bacterium is most likely to appear at old skin. When we analyzed Figure 9C it is possible to note that the presence of *C. kroppenstedtii* is reduced by DF in contrast with the use of CF, that increase their presence. This data indicates that the DF reduce the presence of *C. kroppenstedtii* and the absence of the product (after 30 days = T120) leads to an increase of this bacteria. This data could indicate that the Control Formulation (CF) could stimulate the increase of this bacteria and DF could contribute to maintaining the microbiote balance.

The figure 9D shows the abundance of *C. pseudogenitalium-tuberculostearicum* that is a ubiquitous bacterium that colonizes human skin and is associated with skin inflammation,

according to Altonsy et al. [21]. It is possible to note that DF decrease the abundance of this species, when compared to CF and after 30 days without use DF we could observed that this population shows an increase.

Regarding figure 9E we could observe the abundance of *C. accolens*, whose lipase activity leads to free fatty acid production that can inhibit Streptococcus pneumoniae [22]. It is possible to note that DF increases the amount of this species when compared to the CF and after 30 days without use the abundance decrease. This behavior was not observed for CF formulation.

Regarding the results related to the *Cutibacterium genus*, the *Cutibacterium acnes*, that is related to juvenile skin, is the most abundant, as observed at figure 10A.

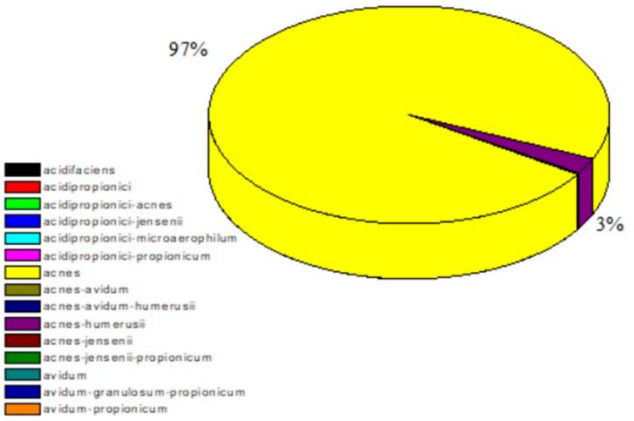

A

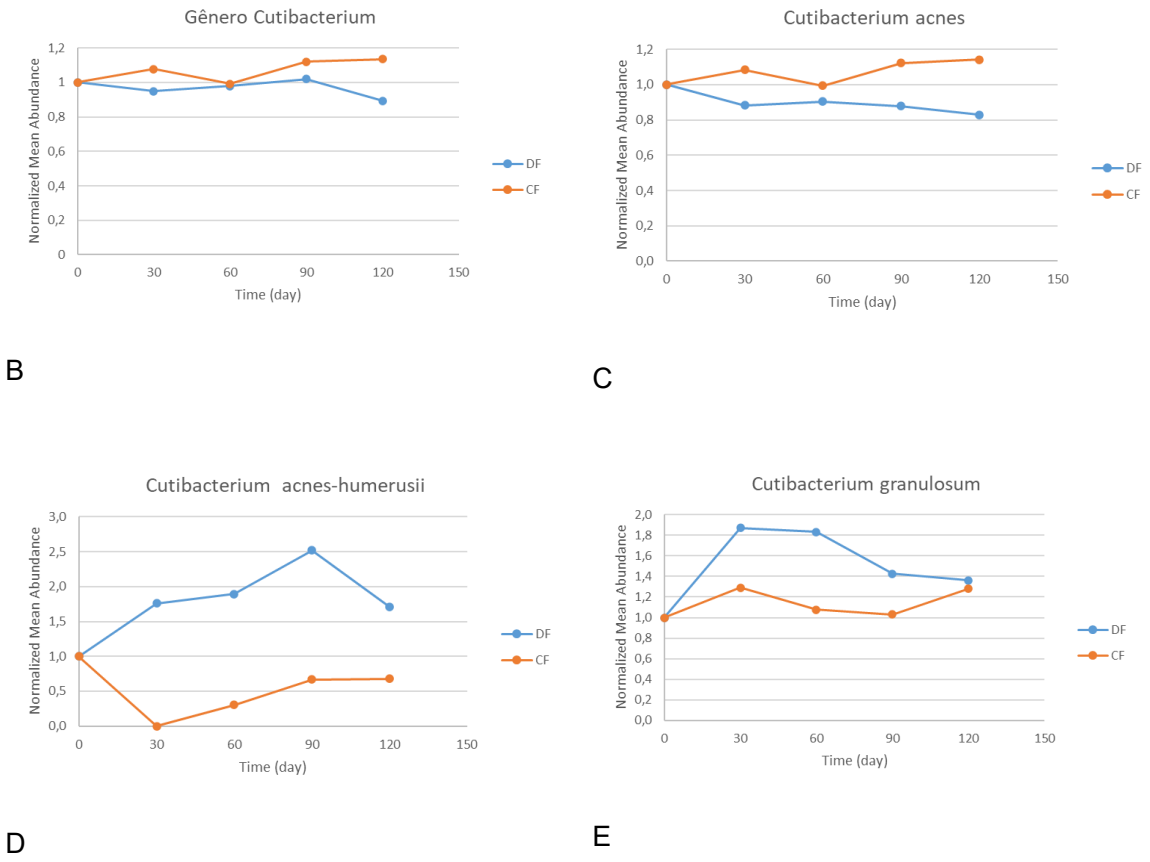

Figure 10. Results from metagenomics analysys regarding *Cutibacterium* sp presence with the most prevalent species. (A). (B) presence of *Cutibacterium* sp Abundance related to DF and CF; (C) presence of *Cutibacterium acnes* abundance related to DF and CF; (D) presence of *Cutibacterium acnes-humerusii* abundance related to DF and CF; (E) presence of *Cutibacterium granulosum* abundance related to DF and CF.

It is possible to observe at figure 10A that the most abundant species is Cutibacterium acnes (97%) at the total population of this genus. At figure 10B it is possible to note a decrease of Cutibaterium genus after 30 days without the use of DF the same comportment observed at figure 10C for the C.acnes. However when we observed figure 10D that report the abundance of C.acnes-humerussi, a not so common species found at the literature, we observed an increase at this population related to the DF use, with a decrease after 30 days without the use. The same comportment was observed for C. granulosum, a species that according to Bronec et al. [23] can secret an endogenous extracellular nuclease, BmdE, that was able to degrade C. acnes biofilm

both in vivo and in vitro, representing a competitive mechanism between two closely related species in the skin. This fact could explain the reduced abundance of C.acnes with the DF formulation.

It is important to emphasis that metabolic end products of C. acnes such as short chain fatty acids (propionate, acetate, butyrate and valerate) might be able to inhibit certain acid-sensitive bacterial strains [24]

5. Conclusion.

This study demonstrated the feasibility of developing a nanostructured cosmetic formulation produced in an economical manner. The results of extensive *in vitro* and *in vivo* tests confirmed the efficacy of the formulation in topical application, showing significant improvements in skin health and appearance. Additionally, the formulation's ability to balance the skin microbiome was proven, indicating potential benefits in combating skin aging.

The presented innovation not only meets the demands for efficacy and safety but also aligns with the needs for sustainability and cost-effectiveness, which are essential for the current cosmetic industry. Based on these findings, the developed formulation holds great potential for market introduction, offering an advanced and affordable solution for skin care. Continuing research and development in this direction may lead to new discoveries and advancements in the field of cosmetics, benefiting both consumers and the industry.

Acknowledgments

We would like to thank Embrapii (Process UNIFESP nº 23089.003494/2023-51) for funding this research.

Conflict of Interest Statement

NONE.

REFERENCES

[1] Grice EA. The skin microbiome: potential for novel diagnostic and therapeutic approaches to cutaneous disease. Semin Cutan Med Surg. 2014; 33:98-103.

[2] Breitwieser FP, Lu J, Salzberg SL. A review of methods and databases for metagenomic classification and assembly. Brief Bioinform 2019; 20(4):1125-36.

[3] Dréno B, Araviiskaia E, Berardesca E, et al. Microbiome in healthy skin, update for dermatologists. J Eur Acad Dermatol 2016; 30:2038-47.

[4] Baldwin HE, Bhatia ND, Friedman A, et al. The role of cutaneous microbiota harmony in maintaining a functional skin barrier. J Drugs Dermatol. 2017; 16(1):12-18.

[5] San Miguel A, Grice EA. Interactions between host factors and the skin microbiome. Cell Mol Life Sci. 2015; 72(8):1499–515.

[6] Berry K, Hallock K, Lam C. Photoaging and Topical Rejuvenation. Facial Plast Surg Clin North Am. 2022; 30(3):291-300.

[7] Salminen A, Kaarniranta K, Kauppinen A. Photoaging: UV radiation-induced inflammation and immunosuppression accelerate the aging process in the skin. Inflamm Res. 2022; 71(7-8):817-31.

[8] Terescenco, D., Picard, C., Clemenceau, F., Grisel, M., & Savary, G. (2018). Influence of the emollient structure on the properties of cosmetic emulsion containing lamellar liquid crystals. Colloids and Surfaces A: Physicochemical and Engineering Aspects, 536, 10–19. https://doi.org/10.1016/j.colsurfa.2017.08.017

[9] Isaac, V. L. B., Cefali, ;, Chiari, ;, Oliveira, ;, Salgado, ;, Corrêa, ;, Lucia, V., & Isaac, B. (2008). Estabilidade físico-química de fitocosméticos Protocolo para ensaios físico-químicos de estabilidade de fitocosméticos. Rev. Ciênc. Farm. Básica Apl., v, 29(1), 81–96.

[10] Castel, V., Rubiolo, A. C., & Carrara, C. R. (2017). Droplet size distribution, rheological behavior and stability of corn oil emulsions stabilized by a novel hydrocolloid (Brea gum) compared with gum arabic. Food Hydrocolloids, 63, 170–177. https://doi.org/10.1016/j.foodhyd.2016.08.039

[11] Glogau RG. Aesthetic and anatomic analysis of the aging skin. Semin Cutan Med Surg. 1996;15(3):134-8.

[12] Perugini, P.; Grignani, C.; Condrò, G.; van der Hoeven, H.; Ratti, A.; Mondelli, A.; Colpani, A.; Bleve, M. Skin Microbiota: Setting up a Protocol to Evaluate a Correlation between the Microbial Flora and Skin Parameters. Biomedicines 2023, 11, 966. https://doi.org/10.3390/biomedicines11030966.

[13] Ferreira, V. T. P., Infante, V. H. P., Felippim, E. C., & Campos, P. M. B. G. M. (2020). Application of Factorial Design and Rheology to the Development of Photoprotective Formulations. AAPS PharmSciTech, 21(2). https://doi.org/10.1208/s12249-019-1569-7

[14] Sougrat R, Morand M, Gondran C, Barré P, Gobin R, Bonté F, Dumas M, Verbavatz JM. Functional expression of AQP3 in human skin epidermis and reconstructed epidermis (2002). J Invest Dermatol. Apr;118(4):678-85. doi: 10.1046/j.1523-1747.2002.01710.x. PMID: 11918716.

[15] Proksch, E. pH in nature, humans and skin (2018). The Journal of Dermatology, Volume45, Issue 9, pages 1044-1052. https://doi.org/10.1111/1346-8138.14489

[16] Berardesca E, Cameli N, Primavera G, Carrera M. Clinical and instrumental evaluation of skin improvement after treatment with a new 50% pyruvic acid peel (2006). Dermatol Surg. Apr;32(4):526-31. doi: 10.1111/j.1524-4725.2006.32106.x. PMID: 16681660.

[17] Henseler H. Investigation of the precision of the Visia® complexion analysis camera system in the assessment of skin surface features (2022). GMS Interdiscip Plast Reconstr Surg DGPW. Nov 29;11:Doc08. doi: 10.3205/iprs000169. PMID: 36567876; PMCID: PMC9762175.

[18] Wang X, Shu X, Li Z, et al. Comparison of two kinds of skin imaging analysis software: VISIA ® from Canfield and IPP® from Media Cybernetics (2018). Skin Res Technol. 00:1–7. https://doi.org/10.1111/srt.12440.

[19] Pequeno ALV, Bagatin E. Dermatological ultrasound in assessing skin aging (2024). Front Med (Lausanne). Feb 12;11:1353605. doi: 10.3389/fmed.2024.1353605. PMID: 38410749; PMCID: PMC10895009.

[20] Garlet, A.; Andre-Frei, V.; Del Bene, N.; Cameron, H.J.; Samuga, A.; Rawat, V.; Ternes, P.; Leoty-Okombi, S. Facial Skin Microbiome Composition and Functional Shift with Aging (2024). *Microorganisms*, *12*, 1021. https://doi.org/10.3390/microorganisms12051021

[21] Altonsy MO, Kurwa HA, Lauzon GJ, et al. Corynebacterium tuberculostearicum, a human skin colonizer, induces the canonical nuclear factor-κB inflammatory signaling pathway in human skin cells (2020). Immun Inflamm Dis. 8:62–79. https://doi.org/10.1002/iid3.284

[22] Horn KJ, Jaberi Vivar AC, Arenas V, Andani S, Janoff EN, Clark SE. Corynebacterium species inhibit Streptococcus pneumoniae colonization and Infection of the Mouse Airway. Front Microbiol. 2022;12:804935.

[23] Bronnec V, Eilers H, Jahns AC, Omer H, Alexeyev OA. Propionibacterium (Cutibacterium) granulosum Extracellular DNase BmdE Targeting Propionibacterium (Cutibacterium) acnes Biofilm Matrix, a Novel Inter-Species Competition Mechanism (2022) Front Cell Infect Microbiol. Jan 13;11:809792. doi: 10.3389/fcimb.2021.809792. PMID: 35155271; PMCID: PMC8834650.

[24] Wang Y, Dai A, Huang S, Kuo S, Shu M, Tapia CP, et al. Propionic acid and its esterified derivative suppress the growth of methicillin-resistant *Staphylococcus aureus (*2014). USA300. Benef Microbes.;5:161–8.